The Ferroxidase Reaction of Ferritin Reveals a Diferric μ-1,2 Bridging Peroxide Intermediate in Common with Other O_2-Activating Non-Heme Diiron Proteins†

Pierre Moënne-Loccoz,*,‡ Carsten Krebs,§ Kara Herlihy,§ Dale E. Edmondson,|| Elizabeth C. Theil,⊥ Boi Hanh Huynh,§ and Thomas M. Loehr‡

Department of Biochemistry and Molecular Biology, Oregon Graduate Institute of Science and Technology, P.O. Box 91000, Portland, Oregon 97291-1000, Departments of Physics, Biochemistry, and Chemistry, Emory University, Atlanta, Georgia 30322, Children's Hospital Oakland Research Institute, 747 52nd Street, Oakland, California 94609

Received January 15, 1999; Revised Manuscript Received March 5, 1999

ABSTRACT: Ferritins are ubiquitous proteins that concentrate, store, and detoxify intracellular iron through oxidation of Fe^{2+} (ferroxidation), followed by translocation and hydrolysis to form a large inorganic mineral core. A series of mutagenesis, kinetics, and spectroscopic studies of ferritin led to the proposal that the oxidation/translocation path involves a diiron protein site. Recent stopped-flow absorption and rapid freeze−quench Mössbauer studies have identified a single peroxodiferric species as the initial transient intermediate formed in recombinant frog M ferritin during rapid ferroxidation [Pereira, S. A., Small, W., Krebs, C., Tavares, P., Edmondson, D. E., Theil, E. C., and Huynh, B. H. (1998) *Biochemistry 37*, 9871−9876]. To further characterize this transient intermediate and to establish unambiguously the peroxodiferric assignment, rapid freeze−quenching was used to trap the initial intermediate for resonance Raman investigation. Discrete vibrational modes are observed for this intermediate, indicating a single chromophore in a homogeneous state, in agreement with the Mössbauer conclusions. The frequency at 851 cm^{-1} is assigned as ν(O−O) of the bound peroxide, and the pair of frequencies at 485 and 499 cm^{-1} is attributed, respectively, to ν_s and ν_{as} of Fe−O_2−Fe. Identification of the chromophore as a μ-1,2 bridged diferric peroxide is provided by the isotope sensitivity of these Raman bands. Similar peroxodiferric intermediates have been detected in a mutant of the R2 subunit of ribonucleotide reductase from *Escherichia coli* and chemically reduced Δ^9 stearoyl-acyl carrier protein desaturase (Δ9D), but in contrast, the ferritin intermediate is trapped from the true reaction pathway of the native protein. Differences in the Raman signatures of these peroxide species are assigned to variations in Fe−O−O−Fe angles and may relate to whether the iron is retained in the catalytic center or released as an oxidized product.

Non-heme dinuclear iron clusters are found in a large number of proteins that utilize O_2 for an array of diverse biological functions. The iron atoms of these proteins reside within a four α-helix bundle structure with Fe···Fe distances ≤ 4 Å and are tethered by one or more bridging carboxylate ligands (*1*−*5*). From this common motif, variations in the geometry and composition of the iron ligands allow the large diversity in function. Hemerythrin (Hr)[1] is an oxygen transport protein in invertebrates (*6*). The two irons are ligated to a total of five histidines and have two bridging carboxylates, and only one open coordination site is available for reversible O_2 binding as a terminal hydroperoxide (*7*, *8*). The evolutionarily distinct diiron enzymes have only two histidines and many more glutamate or aspartate ligands. Four of the ligands occur in a pair of EXXH motifs. In these enzymes, the outer shell of the iron is richer in oxygen, a stronger electron donor than the histidine nitrogen. This may play a role in the reactivity of the cluster toward O_2. Moreover, the versatility of carboxylate coordination (monodentate, bidentate, bridging, and terminal) brings greater flexibility to these metal clusters, making it possible for them to bind O_2 in a bridging fashion. This latter class of diiron enzymes activates and consumes oxygen and includes the R2 subunit of ribonucleotide reductase, the hydroxylase component of soluble methane monooxygenase (MMOH), and Δ^9 stearoyl-acyl carrier protein desaturase (Δ9D) (*1*−*5*, *9*).

Ferritins are ubiquitous proteins that concentrate, store, and detoxify intracellular iron through oxidation of Fe^{2+} (ferroxidation), followed by translocation and hydrolysis to form a large inorganic mineral phase (mineralization) in the protein interior. Crystal structures of ferritins show a spherical arrangement of 24 nearly identical protein subunits forming a hollow complex of ∼480 kDa where up to 4000 Fe^{3+} ions can accumulate (outer diameter ∼120 Å, inner cavity diameter ∼80 Å) (*10*, *11*). Vertebrate ferritins are formed from two different subunits, called H and L, with a

† This work was supported by grants from the NIH (GM-18865 to T.M.L., GM-47295 to B.H.H. and D.E.E., and DK-20251 to E.C.T.) and the NSF (BIR-9216592) for the Raman instrumentation at OGI.

* To whom correspondence should be addressed. E-mail: ploccoz@bmb.ogi.edu.

‡ Oregon Graduate Institute of Science and Technology.

§ Department of Physics, Emory University.

|| Departments of Biochemistry and Chemistry, Emory University.

⊥ Children's Hospital Oakland Research Institute.

[1] Abbreviations: Δ9D, Δ^9 stearoyl-acyl carrier protein desaturase; Hr, hemerythrin; MMOH, hydroxylase component of soluble methane monooxygenase; RR, resonance Raman.

10.1021/bi990095l CCC: $18.00
Published on Web 04/10/1999

tissue-specific stoichiometry that depends on the organism. A third ferritin subunit, an H-subunit isoform, has been identified in frogs and pigs and is designated M because of its electrophoretic mobility (*10, 11*). Regardless of their amino acid sequences, all types of ferritin subunits adopt a four α-helix bundle motif within the 24 subunit complexes (*12*−*15*).

Recent studies with recombinant ferritins have shown that the ferroxidase activity is associated only with H-type subunits which have a ferroxidase site that is lacking in the L subunit. The combination of mutagenesis, kinetic, and spectroscopic studies have identified several conserved residues essential for the ferroxidase activity in H-type ferritins: E23, E58, H61, E103, and Q137[2] (*16*−*22*). In apoferritin, a dinuclear Tb^{3+} (or Ca^{2+}) site, formed with the above-mentioned conserved residues, has been visualized in the crystal structure and proposed as the ferroxidase site (*18*). Two atoms of Fe^{2+} could transiently bind and react with O_2 in this substrate pocket, which would then release the expected products, hydrogen peroxide (*19, 23, 24*) and ferric-oxo (including aqua, hydroxo, and/or oxo) species (*16, 25*−*28*). This proposed diiron site in ferritin contains only one EXXH sequence, distinguishing it from those of the O_2-activating enzymes in which this sequence motif appears twice. Mössbauer and transient absorption spectroscopies have shown that μ-oxo/μ-hydroxo bridged Fe^{3+} dimers are formed as products of the ferroxidase reaction under low iron loading conditions (less than 50 Fe/24-mer ferritin) (*16, 25*−*28*). However, these observations do not directly support formation of an initial diiron protein site since these ferric-oxo species are products of the reaction.

More recently, transient blue species, with absorption at ∼650 nm typical of $O_2^{2-} \rightarrow Fe^{III}$ charge transfer, were reported for ferritin (*21, 29*). Stopped-flow absorption and rapid freeze−quench Mössbauer investigations on the reconstitution of frog M apoferritin (*30, 31*) showed that an intermediate ($\lambda_{max} = 650$ nm, $\epsilon \sim 1000$ M^{-1} cm^{-1}) forms concomitantly with the oxidation of Fe^{2+} and accumulates to a level of 70% of the total iron present (36 Fe/24-mer ferritin). This new species is diamagnetic, and its Mössbauer parameters ($\delta = 0.62$ mm/s, $\Delta E_Q = 1.08$ mm/s) are characteristic of high-spin Fe^{3+}, suggesting an antiferromagnetically coupled diferric system. Because this intermediate forms in parallel with the oxidation of Fe^{2+} and exhibits parameters similar to those of the MMOH (*32*) and D84E R2 (*33*) peroxodiferric intermediates, it was proposed to correspond to the initial peroxo species bound in the ferritin ferroxidase site (*31*).

To further characterize this ferritin intermediate and to establish unambiguously the presence of peroxide bound to the iron atoms, resonance Raman (RR) spectroscopy was used to study the transient species trapped by rapid freeze−quenching. The work reported here represents the first successful RR investigation on a rapid freeze−quenched transient intermediate of a metalloprotein. Discrete vibrational modes are observed for this intermediate, indicating that it is a single chromophore in a homogeneous state. The results confirm the peroxodiferric assignment of this intermediate, in agreement with the previous Mössbauer observation (*31*), and identify this chromophore as a μ-1,2 bridged diferric peroxide. A comparison of the RR signatures of this diiron peroxide in ferritin with those previously observed in a mutant of R2 and in Δ9D (*34, 35*) is presented and related to the role of iron in the function of each of the proteins.

MATERIALS AND METHODS

Recombinant frog M apoferritin (with two or three endogenous iron atoms per molecule of ferritin) was purified as previously reported (*23, 30, 36*). The preparation of samples of the intermediate for RR spectroscopy used rapid freeze−quench procedures similar to those employed previously for the Mössbauer studies (*31, 37*). A major difference is the use of liquid ethane as the quenching cryosolvent rather than the more conventional 2-methylbutane (isopentane). Previous work has shown frozen isopentane to be a strong Raman scatterer that interferes with the detection of weak sample signals. Ethane, with a melting point of −183.2 °C and a boiling point of −88.6 °C, can be maintained in its liquid phase in a cold isopentane bath kept at −155 °C. This temperature is colder than the quenching temperature (−140 °C) normally used with isopentane and ensures a rapid quenching. Liquid ethane is generated by the following procedure: gaseous ethane is condensed into a sample collection apparatus immersed in a bath of liquid nitrogen. The apparatus consists of a glass funnel attached to an EPR tube as previously described (*37*). Under these conditions, ethane freezes inside the tube, which is then transferred to the cold isopentane bath to allow the solid ethane to melt. (Note: ethane and isopentane vapors mixed with air are potentially explosive; all procedures should be carried out with care in a well-ventilated hood.)

An O_2-saturated solution of apoferritin in 0.2 M MOPS buffer (pH 7.0) and 0.2 M NaCl, was mixed at 23 °C with an equal volume of O_2-saturated $FeSO_4$ solution in 3.6 mM H_2SO_4 and 0.2 M NaCl. The final protein concentration after mixing was ∼48 μM (of 24-mer ferritin molecules) with an iron-to-ferritin ratio of ∼36. The reaction of apoferritin with Fe^{2+} in the presence of O_2 was quenched at 25 ms when the accumulation of the peroxodiferric intermediate is maximal and at 4 s when the intermediate has decayed (*31*). The formation of the intermediate in the 25-ms samples was confirmed by the intense blue color of the peroxodiferric species. Oxygen gas isotopes (95 atom % ^{18}O, and 50 atom % ^{18}O) were purchased from ICON Services (Summit, NJ), and the isotope distribution was confirmed by Raman analysis of the gases. Before RR experiments of the proteins, the samples were stored for several days at −80 °C to allow ethane to slowly evaporate. The experimental conditions used for RR spectroscopy are identical to those used in the study of the peroxodiferric species in the R2 mutant (*34*). Spectra were obtained in a backscattering geometry on samples kept at −180 °C with excitation by the 647.1-nm line of a Kr^+ laser (*38*). The laser power at the sample was ∼250 mW. Sequential 30-min exposures were co-added. The similarity of individual spectra and the visual observation of the distinct blue color of the intermediate confirmed the integrity of the sample under laser illumination. A featureless background spectrum was subtracted from the raw data of the intermediate using the 4-s sample as a blank. For this procedure, it was essential that the 25-ms sample and the 4-s blank be

[2] The numbering used in this paper corresponds to the original numbering for ferritin by Rice et al. (*60*), while another commonly used system in the literature differs by +4.

Table 1: Raman Frequencies in Peroxo Complexes[a]

peroxo species	k_{obs} decay rates (s^{-1})	ν_s(M−O)	ν_{as}(M−O)	ν(O−O)	geometry
diiron proteins					
ferritin[b]	4.2	**485** (−17)	**499** (−12)	**851** (−51)	μ-1,2
R2−W48D/D84E[c]	0.26	458 (−16)	499 (−22)	870 (−46)	Fe−O−O−Fe
Δ9D[d]	4.5×10^{-4}	442 (−9)	490 (−19)	898 (−54)	
diiron models					
$[Fe_2(O_2)(N\text{-Et-HPTB})(Ph_3PO)_2](BF_4)_3$[e]		476 (−16)	nr	900 (−50)	cis μ-1,2
$[Fe_2O(O_2)(6\text{-}Me_3\text{-TPA})_2](ClO_4)_2$[f]		462 (−21)	nr	848 (−46)	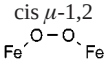
$[Fe_2(O_2)(\mu\text{-}O_2CCH_2Ph)_2(HB(pz')_3)_2]$[g]		415 (−11)	nr	888 (−46)	gauche μ-1,2 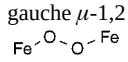
dicopper systems					
$[Cu_2(UN{-}O^-)(O_2H)](PF_6)_2$[h]		322 (−10)	506 (−15)	892 (−52)	μ-1,1 
oxyhemocyanin[i]		*j*	542 (−23)	749 (−40)	μ-η^2:η^2 

[a] Frequencies in cm^{-1}; $^{18}O_2$ isotope shifts in parentheses; nr = not reported. [b] This work. [c] Data from ref 34. [d] Data from ref 35. [e] Data from ref 40. [f] Data from ref 51. [g] Data from ref 50. Although no crystal structure is available, similar frequencies of 421 (−12), nr, and 876 (−48) cm^{-1}, respectively, have been observed for the corresponding μ-benzoate complex (*56*). [h] Data from ref 59. [i] *Octopus dofleini* oxyhemocyanin data from ref 45. [j] The $\nu_s(Cu_2O_2)$ modes are admixed with Cu−N(His) modes (*45*).

prepared during the same freeze−quench experiment and that their spectra be obtained successively using identical data collection settings.

RESULTS AND DISCUSSION

The resonance Raman spectrum of the blue intermediate in M ferritin prepared with $^{16}O_2$ has a band at 851 cm^{-1} and a low-frequency band that can be deconvoluted into two Gaussians at 485 and 499 cm^{-1} in an ∼2:1 intensity ratio (Figure 1). The presence of these distinct RR bands with typical bandwidths of 15−20 cm^{-1} demonstrates that the broad 650-nm electronic transition corresponds to a unique chromophore in a homogeneous environment. The 851-cm^{-1} band is within the expected range for the O−O stretch of a metal-coordinated peroxide (*38*, *39*). It is shifted by −51 cm^{-1} to 800 cm^{-1} when pure $^{18}O_2$ gas is used to form the intermediate (Figure 1 and Table 1). The magnitude of this isotope shift agrees well with the calculated value for a diatomic oscillator (−49 cm^{-1}).

Additional information about the peroxo species was obtained using a mixed-isotope gas composed of 25% $^{16}O_2$, 50% $^{16}O^{18}O$, and 25% $^{18}O_2$. The intermediate produced by this mixture shows an unresolved group of bands in the 775−875-cm^{-1} region. The maximum intensity lies between the $^{16}O-^{16}O$ and $^{18}O-^{18}O$ frequencies at 851 and 800 cm^{-1}, respectively (Figure 1), a result consistent with the presence of ∼50% of $^{16}O-^{18}O$ peroxide. However, the exact frequency of the mixed-isotope species is difficult to determine. In our previous studies of peroxodiferric complexes in R2 and Δ9D (*34*, *35*), the ν(O−O) spectral region in the mixed-isotope experiment showed high discrimination between the different spectral components. In contrast, ferritin displays an unstructured cluster of bands. This may be explained by the larger intrinsic bandwidths of ν(O−O) bands in ferritin as compared to R2 and Δ9D, resulting in greater overlap between the individual spectral contributions in the mixed-isotope experiments. Moreover, Fermi resonance splitting may induce further broadening of the signal. Such splittings,

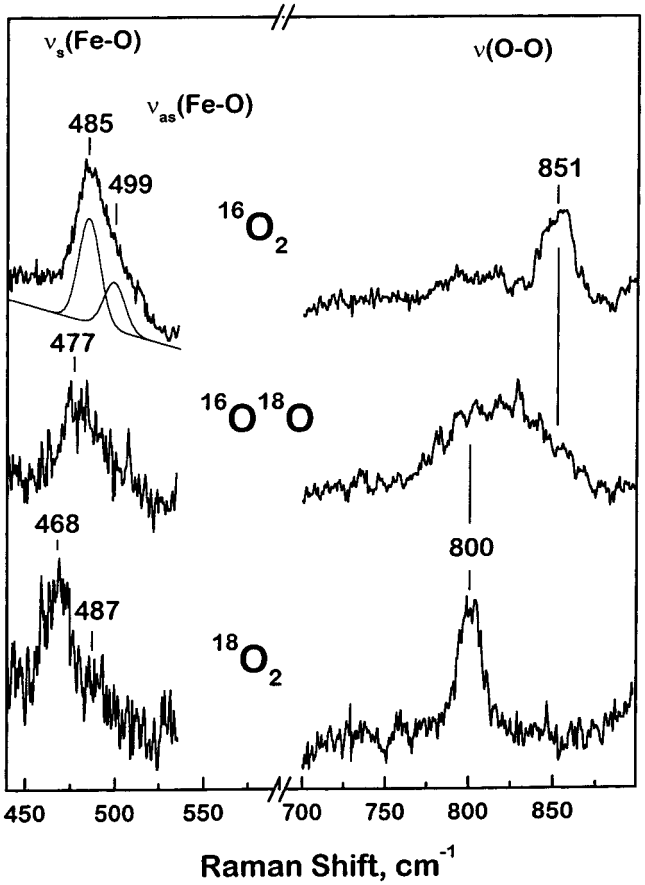

FIGURE 1: Resonance Raman spectra of the rapid (25 ms) freeze-quenched peroxodiferric intermediate in frog M ferritin generated with (top) $^{16}O_2$, (middle) 50 atom % ^{18}O containing 50% $^{16}O^{18}O$, 25% $^{16}O_2$, and 25% $^{18}O_2$, and (bottom) $^{18}O_2$ gas.

also observed in the RR spectra of the $^{17}O_2$−peroxo complex of R2 and the $^{18}O_2$−peroxo complex of Δ9D, are proposed to involve coupling of O−O stretches with a nonresonant vibration at ∼845 cm^{-1} common to these diiron clusters (*34*, *35*). It is likely that the $\nu(^{16}O-^{16}O)$ and $\nu(^{16}O-^{18}O)$ in ferritin are somewhat broadened by such vibrational mixing. Similar

splittings have also been observed in peroxodiferric model compounds (*40, 41*).

In the low-frequency region, two bands are observed at 485 and ~499 cm^{-1} in the $^{16}O_2$ sample that appear to be downshifted by 17 and ~12 cm^{-1}, respectively, in the $^{18}O_2$ sample (Figure 1 and Table 1). These frequencies are consistent with Fe−O stretches (*38, 39*). The observed shift of the more intense band compares reasonably well with the calculated value of −21 cm^{-1} for an Fe−O diatomic oscillator. However, the exact shift of the minor component is uncertain. The frequency and intensity pattern of these two bands suggest their assignment to symmetric and antisymmetric Fe−O stretching modes, as expected for a peroxo group coordinating two ferric iron atoms in a *bridging* fashion (Table 1). This interpretation is consistent with the mixed-isotope experiment that displays a broad RR signal with maximum intensity at ~477 cm^{-1} (Figure 1). Because the position of this maximum is midway between the ^{16}O and ^{18}O ν_s(Fe−O) and the predominant species in the sample is the $^{16}O^{18}O$ peroxide, we assign the 477-cm^{-1} maximum to the ν_s(Fe−O) of a symmetrically bridged mixed-isotope peroxo species.[3] The present data do not support an asymmetric binding of $^{16}O^{18}O$ in a μ-1,1 geometry which would be expected to exhibit extreme broadening or even splitting of the ν(Fe−O) feature toward the positions of the Fe−$^{16}O_2$ or Fe−$^{18}O_2$ frequencies. Such splitting has been seen in the asymmetric peroxo adduct of a dicopper compound (*42*) and the end-on bound O_2 of oxyHr (*43*). It is also worth noting that the only well-characterized μ-1,1 complex shows a very low ν_s(Cu−O) (Table 1). The symmetric binding mode of the peroxo ligand deduced from the RR data is also consistent with the Mössbauer study (*31*).

Symmetrically bridged O−O complexes may possess μ-1,2 or μ-η^2:η^2 geometries. The latter, also known as side-on bridging, has thus far not been observed with iron. However, in oxyhemocyanin (*44, 45*), oxytyrosinase (*46*), and several copper complexes (*47*−*49*) in which μ-η^2:η^2 coordination of O_2 is seen, significantly lower O−O stretching frequencies are observed than for the ferritin intermediate (Table 1). The RR frequencies observed in the ferritin peroxide fit well with those observed in μ-1,2 diferric peroxide model compounds (*40, 50, 51*). Moreover, one should note the striking similarity of the RR signatures, including the number of modes, frequencies, isotope sensitivities, and relative intensities of the peroxo species in ferritin, R2 (*34*), and Δ9D (*35*) (Table 1).

The relatively high stabilities of the peroxo species in R2−W48F/D84E and chemically reduced Δ9D raised some concerns regarding their participation as intermediates in the physiological reactions of these enzymes. *In contrast, the ferritin intermediate reported in this paper is trapped from the true reaction pathway of the native protein*. We have noticed an interesting correlation between the O−O and the Fe−O stretching frequencies of these different peroxo species. As the O−O stretching frequencies increase, the corresponding Fe−O stretching frequencies decrease (Table 1). These trends may reflect variations in the geometry of these peroxide units. In μ-oxo-bridged diiron systems, a clear correlation has been established between the symmetric and asymmetric Fe−O−Fe stretching frequencies and the Fe−O−Fe angles (*52*). By analogy, in the Fe−O−O−Fe systems the vibrational modes may also correlate with bond angles. Recently, Brunold et al. published an extensive spectroscopic and theoretical study of a diferric cis μ-1,2 peroxide model compound (*53*). From a normal-coordinate analysis of the Fe−O−O−Fe unit, these authors proposed that the Fe−O and O−O stretching frequencies are mechanically coupled and strongly dependent on the Fe−O−O angle.[4] The calculation predicts decreasing ν(O−O) and increasing ν(Fe−O) as the Fe−O−O angle gets smaller with insignificant changes in the O−O bond strength (*53*). This theoretical approach also predicts that the ν(O−O) is not influenced by the Fe−O−O−Fe dihedral angle but that the ν(Fe−O) increases by ~90 cm^{-1} upon cis → trans conversion (*53*). Relating our data to their analysis and assuming a *cis*-planar orientation for the Fe−O−O−Fe unit, the observed RR frequencies suggest Fe−O−O angles of ~110°, 125°, and 140° for the peroxide intermediates in ferritin, R2, and Δ9D, respectively.

We also note that the lower the ν(O−O) frequency, the faster the μ-1,2 peroxide decays (Table 1), suggesting a correlation between Fe−O−O−Fe angles and reactivity. Symmetric μ-1,2 bridging peroxide intermediates appear as likely precursors to O−O bond cleavage. Wild-type R2 reacts with O_2 to form intermediate X, which can be described as a spin-coupled formally Fe^{III}/Fe^{IV} cluster containing a μ-oxo and a terminal aqua ligand derived from O_2 (*54, 55*). In MMOH, a bis(μ-oxo) diamond core geometry is believed to occur at the Fe^{IV}/Fe^{IV} level (*56*). The transition from a μ-1,2 peroxo to a diamond core or to a μ-oxo-plus-a-terminal-water-ligand structure is likely to strongly depend on Fe−O−O−Fe angles. However, the species formed after the peroxide observed in R2−W48F/D84E and chemically reduced Δ9D are not known. The next intermediate in the ferroxidase reaction of ferritin is also unknown, although oxo-bridged ferric dimers and trimers have been observed by Mössbauer spectroscopy (*28*), and H_2O_2 is detected as the primary product (*19, 23, 24*). The decay mechanism of the peroxide intermediate may involve protonation of the bound peroxide followed by release of H_2O_2 and oxidized iron. Alternatively, the peroxide may decay, via O−O bond cleavage, to a high-valent intermediate which reacts with water to form the observed products (*31*).

[3] A more thorough analysis of this region of the spectrum needs to consider the summation of the contributions from the $^{16}O_2$, $^{16}O^{18}O$, and $^{18}O_2$ intermediates formed, which implies a minimum of six bands. Whereas it is unrealistic to attempt to deconvolute such a complex cluster of bands, it is important to check that it fits with our working model. Therefore, the envelope of the mixed isotope signal was fitted with 6 Gaussians of fixed bandwidths (14 cm^{-1}, deduced from the pure isotope spectra), fixed intensities (2:1 for ν_s:ν_{as} of the species produced from pure isotopes, and 2× (2:1) for the mixed-isotope species), and fixed frequencies for the $^{16}O_2$ and $^{18}O_2$ contributions. The only free parameters are the two frequencies of the expected bands of the $^{16}O^{18}O$ species. The best fit is obtained when these two contributions are positioned at ~477 and 492 cm^{-1}, in full agreement with a μ-1,2 bridging peroxide (Table 1).

[4] As in our RR data on enzyme intermediates, the model compound studied by Brunold et al. (*53*) shows good agreement between the observed oxygen-isotope sensitivity of the O−O stretch and the calculated value for an isolated diatomic oscillator. The authors explain that the coupling of ν(O−O) with ν(Fe−O) is not reflected in the ν(O−O) isotope sensitivity because the ν(Fe−O) mostly involves displacement of the oxygen atom.

For ferritin, iron is a substrate, and after its oxidation at the ferroxidase site it is most likely released and translocated to the inner protein cavity to form the mineral core. The observation of similar peroxodiferric intermediates in ferritin and O_2-activating diiron enzymes suggests a common mechanism for the initial reactions of oxygen with these proteins. The distinctive RR signatures and Mössbauer quadrupole splittings of the peroxodiferric complexes in each protein may reflect geometrical variations influenced by their protein ligands. Although similar, the ligand environment of the diiron site in ferritin is different from those in R2 and Δ9D. For example, the sequence EXXH occurs twice at the diiron sites in R2 and Δ9D but only once in H-type ferritins. The missing histidine ligand is replaced by a glutamine in one of the ferric sites and a second carboxylate bridge, observed in ferrous R2 (*57*), is absent (*18*). Effects of these structural differences on the stability of the peroxide intermediates are not known but in *E. coli* ferritin (FtnA), which has a histidine at the second iron site (ExHxxE), the initial ferric species decays much more slowly than in H-type eukaryotic ferritins (*58*).

ACKNOWLEDGMENT

We thank William Small for purification of the frog M ferritin used in this study and Joann Sanders-Loehr and Lawrence Que, Jr., for helpful discussions.

REFERENCES

1. Feig, A. L., and Lippard, S. J. (1994) *Chem. Rev. 94*, 759−805.
2. Nordlund, P., and Eklund, H. (1995) *Curr. Opin. Struct. Biol. 5*, 758−766.
3. Wallar, B. J., and Lipscomb, J. D. (1996) *Chem. Rev. 96*, 2625−2657.
4. Kurtz, D. M., Jr. (1997) *J. Biol. Inorg. Chem. 2*, 159−167.
5. Fox, B. G. (1997) in *Comprehensive Biological Catalysis* (Sinnott, M., Ed.), pp 261−348, Academic Press, London.
6. Stenkamp, R. E. (1994) *Chem. Rev. 94*, 715−726.
7. Stenkamp, R. E., Sieker, L. C., Jensen, L. H., McCallum, J. D., and Sanders-Loehr, J. (1985) *Proc. Natl. Acad. Sci. U.S.A. 82*, 713−716.
8. Holmes, M. A., Le Trong, I., Turley, S., Sieker, L. C., and Stenkamp, R. E. (1991) *J. Mol. Biol. 218*, 583−593.
9. Que, L., Jr., and Dong, Y. (1996) *Acc. Chem. Res. 29*, 190−196.
10. Waldo, G. S., and Theil, E. C. (1996) in *Comprehensive Supramolecular Chemistry* (Suslick, K. S., Ed.) Vol. 5, pp 65−89, Pergamon Press, Oxford.
11. Harrison, P. M., and Arosio, P. (1996) *Biochim. Biophys. Acta 1275*, 161−203.
12. Frolow, F., Kalb (Gilboa), A. J., and Yariv, J. (1994) *Struct. Biol. 1*, 453−460.
13. Trikha, J., Waldo, G. S., Lewandowski, F. A., Ha, Y., Theil, E. C., Weber, P. C., and Allewell, N. M. (1994) *Proteins 18*, 107−118.
14. Trikha, J., Theil, E. C., and Allewell, N. M. (1995) *J. Mol. Biol. 248*, 949−967.
15. Hempstead, P. D., Yewdall, S. J., Fernie, A. R., Lawson, D. M., Artymiuk, P. J., Rice, D. W., Ford, G. C., and Harrison, P. M. (1997) *J. Mol. Biol. 268*, 424−448.
16. Bauminger, E. R., Harrison, P. M., Hechel, D., Nowik, I., and Treffry, A. (1991) *Biochim. Biophys. Acta 1118*, 48−58.
17. Wade, V. J., Levi, S., Arosio, P., Treffry, A., Harrison, P. M., and Mann, S. (1991) *J. Mol. Biol. 221*, 1443−1452.
18. Lawson, D. M., Artymiuk, P. J., Yewdall, S. J., Smith, J. M., Livingstone, J. C., Treffry, A., Luzzago, A., Levi, S., Arosio, P., Cesareni, G., Thomas, C. D., Shaw, W. V., and Harrison, P. M. (1991) *Nature 349*, 541−544.
19. Sun, S., Arosio, P., Levi, S., and Chasteen, N. D. (1993) *Biochemistry 32*, 9362−9369.
20. Hempstead, P. D., Hudson, A. J., Artymiuk, P. J., Andrews, S. C., Banfield, M. J., Guest, J. R., and Harrison, P. M. (1994) *FEBS Lett. 350*, 258−262.
21. Treffry, A., Zhao, Z., Quail, M. A., Guest, J. R., and Harrison, P. M. (1995) *Biochemistry 34*, 15204−15213.
22. Treffry, A., Zhao, Z., Quail, M. A., Guest, J. R., and Harrison, P. M. (1997) *Biochemistry 36*, 432−441.
23. Waldo, G. S., and Theil, E. C. (1993) *Biochemistry 32*, 13262−13269.
24. Yang, X., Chen-Barrett, Y., Arosio, P., and Chasteen, N. D. (1998) *Biochemistry 37*, 9743−9750.
25. Bauminger, E. R., Harrison, P. M., Nowik, I., and Treffry, A. (1989) *Biochemistry 28*, 5486-5493.
26. Treffry, A., Hirzmann, J., Yewdall, S. J., and Harrison, P. M. (1992) *FEBS Lett. 302*, 108−112.
27. Bauminger, E. R., Harrison, P. M., Hechel, D., Hodson, N. W., Nowik, I., Treffry, A., and Yewdall, S. J. (1993) *Biochem. J. 296*, 709−719.
28. Pereira, A. S., Tavares, P., Lloyd, S. G., Danger, D., Edmondson, D. E., Theil, E. C., and Huynh, B. H. (1997) *Biochemistry 36*, 7917−7927.
29. Zhao, Z., Treffry, A., Quail, M. A., Guest, J. R., and Harrison, P. M. (1997) *J. Chem. Soc., Dalton Trans.*, 3977−3978.
30. Fetter, J., Cohen, J., Danger, D., Sanders-Loehr, J., and Theil, E. C. (1997) *J.Biol. Inorg. Chem. 2*, 652−661.
31. Pereira, A. S., Small, W., Krebs, C., Tavares, P., Edmondson, D. E., Theil, E. C., and Huynh, B. H. (1998) *Biochemistry 37*, 9871−9876.
32. Liu, K. E., Valentine, A. M., Wang, D., Huynh, B. H., Edmondson, D. E., Salifoglou, A., and Lippard, S. J. (1995) *J. Am. Chem. Soc. 117*, 10174−10185.
33. Bollinger, J. M., Jr., Krebs, C., Vicol, A., Chen, S., Ley, B. A., Edmondson, D. E., and Huynh, B. H. (1998) *J. Am. Chem. Soc. 120*, 1094−1095.
34. Moënne-Loccoz, P., Baldwin, J., Ley, B. A., Loehr, T. M., and Bollinger, J. M., Jr. (1998) *Biochemistry 37*, 14659−14663.
35. Broadwater, J. A., Ai, J., Loehr, T. M., Sanders-Loehr, J., and Fox, B. G. (1998) *Biochemistry 37*, 14664−14671.
36. Waldo, G. S., Ling, J., Sanders-Loehr, J., and Theil, E. C. (1993) *Science 259*, 796−798.
37. Ravi, N., Bollinger, J. M., Jr., Huynh, B. H., Edmondson, D. E., and Stubbe, J. (1994) *J. Am. Chem. Soc. 116*, 8007−8014.
38. Loehr, T. M., and Sanders-Loehr, J. (1993) *Methods Enzymol. 226*, 431−470.
39. Nakamoto, K. (1997) *Infrared and Raman Spectroscopy of Inorganic and Coordination Compounds*, 5th ed., John Wiley and Sons, Inc., New York.
40. Dong, Y., Menage, S., Brennan, B. A., Elgren, T. E., Jang, H. G., Pearce, L. L., and Que, L., Jr. (1993) *J. Am. Chem. Soc. 115*, 1851−1859.
41. Dong, Y., Yan, S., Young, V. G., Jr., and Que, L., Jr. (1996) *Angew. Chem., Int. Ed. Engl. 35*, 618−620.
42. Pate, J. E., Cruse, R. W., Karlin, K. D., and Solomon, E. I. (1987) *J. Am. Chem. Soc. 109*, 2624−2630.
43. Kurtz, D. M., Jr., Shriver, D. F., and Klotz, I. M. (1976) *J. Am. Chem. Soc. 98*, 5033−5035.
44. Magnus, K. A., Hazes, B., Ton-That, H., Bonaventura, C., Bonaventura, J., and Hol, W. G. J. (1994) *Proteins 19*, 302−309.
45. Ling, J., Nestor, L. P., Czernuszewicz, R. S., Spiro, T. G., Fraczkiewicz, R., Sharma, K. D., Loehr, T. M., and Sanders-Loehr, J. (1994) *J. Am. Chem. Soc. 116*, 7682−7691.
46. Baldwin, M. J., Root, D. E., Pate, J. E., Fujisawa, K., Kitajima, N., and Solomon, E. I. (1992) *J. Am. Chem. Soc. 114*, 10421−10431.
47. Kitajima, N., Fujisawa, K., Fujimoto, C., Moro-oka, Y., Hashimoto, S., Kitagawa, T., Toriumi, K., Tatsumi, K., and Nakamura, A. (1992) *J. Am. Chem. Soc. 114*, 1277−1291.

48. Mahapatra, S., Halfen, J. A., Wilkinson, E. C., Que, L., Jr., and Tolman, W. B. (1994) *J. Am. Chem. Soc. 116*, 9785−9786.
49. Pidcock, E., Obias, H. V., Zhang, C. X., Karlin, K. D., and Solomon, E. I. (1998) *J. Am. Chem. Soc. 120*, 7841−7847.
50. Kim, K., and Lippard, S. J. (1996) *J. Am. Chem. Soc. 118*, 4914−4915.
51. Dong, Y., Zang, Y., Shu, L., Wilkinson, E. C., and Que, L., Jr. (1997) *J. Am. Chem. Soc. 119*, 12683−12684.
52. Sanders-Loehr, J., Wheeler, W. D., Shiemke, A. K., Averill, B. A., and Loehr, T. M. (1989) *J. Am. Chem. Soc. 111*, 8084−8093.
53. Brunold, T. C., Tamura, N., Kitajima, N., Moro-oka, Y., and Solomon, E. I. (1998) *J. Am. Chem. Soc. 120*, 5674−5690.
54. Sturgeon, B. E., Burdi, D., Chen, S., Huynh, B.-H., Edmondson, D. E., Stubbe, J., and Hoffman, B. M. (1996) *J. Am. Chem. Soc. 118*, 7551−7557.
55. Burdi, D., Willems, J.-P., Riggs-Gelasco, P., Antholine, W. E., Stubbe, J., and Hoffman, B. M. (1998) *J. Am. Chem. Soc. 120*, 12910−12919.
56. Shu, L., Nesheim, J. C., Kauffmann, K., Münck, E., Lipscomb, J. D., and Que, L., Jr. (1997) *Science 275*, 515−518.
57. Logan, D. T., Su, X. D., Åberg, A., Regnström, K., Hajdu, J., Eklund, H., and Nordlund, P. (1996) *Structure 4*, 1053−1064.
58. Treffry, A., Zhao, Z., Quail, M. A., Guest, J. R., and Harrison, P. M. (1998) *FEBS Lett. 432*, 213−218.
59. Root, D. E., Mahroof-Tahir, M., Karlin, K. D., and Solomon, E. I. (1998) *Inorg. Chem. 37*, 4838−4848.
60. Rice, D. W., Ford, G. C., White, J. L., Smith, J. M. A., and Harrison, P. M. (1983) *Adv. Inorg. Biochem. 5*, 39−50.

BI990095L